Chem. Mater. **2007,** *19,* 3127−3138

Characterization of Ultra-Thin Hafnium Oxide Films Grown on Silicon by Atomic Layer Deposition Using Tetrakis(ethylmethyl-amino) Hafnium and Water Precursors

Y. Wang, M.-T. Ho, L. V. Goncharova, L. S. Wielunski, S. Rivillon-Amy, Y. J. Chabal,* and T. Gustafsson

Laboratory for Surface Modification, Rutgers University, Piscataway, New Jersey 08854

N. Moumen

SEMATECH, 2706 Montopolis Drive, Austin, Texas 78741

M. Boleslawski

SAFC, 5485 Country Road, Sheboygan Falls, Wisconsin 53085

Received July 27, 2006. Revised Manuscript Received April 16, 2007

The role and effectiveness of chemical pre-functionalization of silicon surfaces (with hydrogen, chlorine, and nitride) to minimize interfacial SiO_2 formation during atomic layer deposition growth has been investigated using in situ transmission infrared spectroscopy, ex situ Rutherford backscattering spectroscopy, and ex situ medium energy ion scattering spectroscopy. No measurable SiO_2 was formed during growth at low temperatures (∼100 °C) with tetrakis(ethylmethylamino) hafnium and heavy water as precursors on H-, Cl-, and nitride-passivated silicon surfaces. Interfacial SiO_2 appeared after postdeposition annealing, at the point when the initially amorphous HfO_2 film crystallized, as reflected by the appearance of a monoclinic HfO_2 phonon peak at ∼780 cm^{-1} and by a periodic arrangement of atoms observed in high-resolution transmission electron microscopic images. Electrical characterization of as-deposited HfO_2 films showed that, while the interfacial defect density was reasonably low at growth temperatures when interfacial hydrogen was still present (∼100 °C), the leakage current was significantly increased after postdeposition annealing (∼700 °C in nitrogen).

Introduction

The growth of the silicon semiconductor industry in the past few decades has largely been driven by the improvement of integrated circuits (IC) based on metal-oxide-semiconductor field effect transistor (MOSFET) technology. Silicon has remained the dominant material for MOSFET devices mainly due to the stability and excellent dielectric and electrical properties of its oxide,[1] such as a wide band gap (9 eV), low interface state density ($<5 \times 10^{10}$ states/eV cm^2), and stability over a wide range of thermal and electrical stress conditions. However, further scaling of the MOSFET gate dielectric (SiO_2) thickness has now reached a point where the quantum mechanical tunneling current is unacceptable.[2] To maintain a high MOSFET gate capacitance (i.e., good drive current) with minimal power loss, high-κ dielectrics such as HfO_2 ($\kappa = 25$) and Al_2O_3 ($\kappa = 9$)[3] are being considered seriously.[4,5] Their use is, however, hindered by the formation of an interfacial SiO_2 layer in the high-κ/Si stack, significantly increasing the equivalent oxide thickness (EOT), and thus partially compromising the benefit of high-κ oxide by reducing the effective gate capacitance.[6,7] In this article, we discuss efforts to minimize the SiO_2 interfacial layer for the HfO_2/Si stack by chemical pretreatment of silicon surfaces prior to HfO_2 deposition.

Atomic layer deposition (ALD) is a technique[8] that allows conformal growth of thin films over large surface areas, and even for surfaces with high aspect ratio features, the use of high-κ materials is a realistic possibility.[9] Typically, high-κ oxide ALD is based on the use of two precursors, such as metal halogenides or organometallic molecules and an oxidizing agent, serving as the metal and oxygen sources, respectively.[8] A distinctive feature of ALD as compared to other film deposition techniques is the self-limiting adsorp-

* Corresponding author. Tel.: (732) 445-8248; fax: (732) 445-4991; e-mail: yves@agere.rutgers.edu.

(1) Green, M. L.; Gusev, E. P.; Degraeve, R.; Garfunkel, E. L. *J. Appl. Phys.* **2001**, *90*, 2057.
(2) Choi, C.-H.; Nam, K.-Y.; Yu, Z.; Dutton, R. W. *IEEE Trans. Electron Devices* **2001**, *48* (12), 2823.
(3) Wilk, G. D.; Wallace, R. M.; Anthony, J. M. *J. Appl. Phys.* **2001**, *89*, 5243.
(4) Kingon, A. I.; Maria, J.-P.; Streiffer, S. K. *Nature* **2000**, *406*, 1032.
(5) Park, D.-G.; Cho, H.-J.; Lim, K.-Y.; Lim, C.; Yeo, I.-S.; Roh, J.-S.; Park, J. W. *J. Appl. Phys.* **2001**, *89*, 6275.
(6) Scarel, G.; Spiga, S.; Wiemer, C.; Tallarida, G.; Ferrari, S.; Fanciulli, M. *Mater. Sci. Eng., B* **2004**, *109*, 11.
(7) Chowdhuri, A. R.; Takoudis, C. G.; Klie, R. F.; Browning, N. D. *Appl. Phys. Lett.* **2002**, *80*, 4241.
(8) (a) Ritala, M.; Leskelä, M. Atomic layer deposition. In *Handbook of Thin Film Materials*; Nalwa, H. S., Ed.; Academic Press: San Diego, 2002; Vol. 1, Ch. 2, p 103. (b) Puurunen, R. *J. Appl. Phys.* **2005**, *97*, 121301.
(9) Hausmann, D.; Becker, J.; Wang, S.; Gordon, R. G. *Science* **2002**, *298*, 402.

10.1021/cm061761p CCC: $37.00 © 2007 American Chemical Society
Published on Web 06/05/2007

tion behavior of each precursor. This self-limiting property makes it possible to control the growth at the atomic layer level. To avoid cross-reactions between the two gas-phase precursors (as is the case for CVD processes), an inert gas purge separates each precursor pulse. As a result, each precursor can only react with the chemisorbed species of the previous precursor, eliminating organic ligands in the reaction. A uniform film with its thickness controlled by the number of ALD cycles can thus be formed regardless of the initial surface morphology. However, the chemical quality of the film depends on the choice of precursor and growth conditions.

Despite the recent interest of ALD in the industry,[10] the surface and interface reaction mechanisms are not well-understood. This is partially due to the lack of in situ surface characterization techniques to monitor the surface reactions during the initial stages of the ALD process.[11] Transmission infrared (IR) spectroscopy is well-suited to study the surface chemistry on single-crystal surfaces[12] and has been used here to identify the presence and formation mechanism of interfacial SiO_2. Other ex situ surface/interface characterization techniques such as Rutherford backscattering spectroscopy (RBS), medium energy ion scattering spectroscopy (MEIS), and high-resolution transmission electron microscopy (HRTEM) can also be used to provide elemental and structural information not readily available with IR spectroscopy.

In this paper, we explore the mechanisms involved in interface formation during ALD growth of HfO_2 on Si with different chemical terminations, with a specific focus on understanding the formation of interfacial SiO_2. We first describe the methods used for functionalizing the surface prior to ALD growth that are believed to help minimize interfacial SiO_2 growth. We then discuss the characterization techniques and the ALD growth experiments. In the case of ultra-thin film (<2 nm) deposition, we show that the starting surface termination affects the film growth linearity and the overall properties of the dielectric layer. Since the structure and composition of the interfacial layer depend on the early stages of film growth, the focus of this work is therefore on the surface evolution during the first 5 ALD cycles. Film contamination issues are also discussed since the electrical properties of the high-κ dielectrics can be affected by contaminants such as hydrocarbons, chlorine, and hydroxyl groups.[13,14]

Experimental Procedures

Silicon Surface Chemical Functionalization. Silicon substrates (3.8 cm × 1.5 cm) were cut from double-side polished, lightly doped Si(111) and Si(100) wafers (Virginia Semiconductor, $\rho = \sim 10\ \Omega$ cm). Prior to the HfO_2 film deposition, all samples were rinsed in acetone and ethanol followed by standard RCA cleaning to remove organic and metallic contaminants.[15] The substrates were therefore passivated with a thin oxide layer (referred to as RCA SiO_2) and acted as templates for HfO_2 ALD. The oxidized (hydroxyl-terminated) Si wafers were mounted in the ALD reactor. For technical reasons, the surface hydroxyl groups were replaced by OD groups by D_2O exposure prior to the ALD process.

H-terminated Si surfaces (H/Si) were prepared by 1 min HF (~20%, J. T. Baker) etching for Si(100) and an additional 2 min NH_4F (~49%, J. T. Baker) etching for Si(111) surfaces.[16,17] H/Si-(100) is atomically rough with at least one double layer (~3−4 Å) roughness,[18] while H/Si(111) is atomically flat, making it possible to distinguish intrinsic surface reactions from extrinsic effects due to surface defects.

Chlorination of atomically flat H/Si(111) was performed ex situ at atmospheric pressure in a stainless steel reactor that was continuously purged with ultra-pure nitrogen (N_2 (g), O_2 impurities < 10^{-6} ppm). Chlorine gas (Cl_2 (g), Matheson, 99.999%) was introduced with purified N_2 carrier gas ($Cl_2/N_2 = 0.3\%$, total flow rate = 4.7 L/min), while the chlorination reactor was maintained at 95 ± 2 °C for 1 h during Cl_2 (g) exposure. After gas-phase chlorination, the reactor was purged with purified N_2 (g) for 30 min before unloading the sample from the reaction chamber. The Cl/Si substrate was immediately transferred into the N_2 purged ALD chamber and examined with transmission IR prior to HfO_2 film deposition.

An ultra-thin layer of silicon nitride (Si_xN_y) for Si substrate passivation was prepared in situ in the ALD chamber by exposing H/Si to ammonia gas (NH_3 (g), 99.999%, Messer) at 500 °C for 2 min at ~5 Torr. To minimize residual water and oxygen from the reactor chamber walls, a moderate temperature (~200−300 °C) anneal was performed in NH_3 for 2 min prior to the 500 °C treatment.

Hafnium Oxide ALD and Postannealing. ALD of HfO_2 was performed by introducing tetrakis(ethylmethyl-amino) hafnium ($Hf-N_4(CH_3)_4(C_2H_5)_4$ or TEMAH, 99.99%, Sigma-Aldrich) and deuterium oxide (D_2O, 99.990 atom % D, Sigma-Aldrich) vapors alternately onto the prefunctionalized silicon substrates. D_2O was used in place of H_2O to avoid interference in the IR spectrum from H_2O vapors in the spectrometer during IR measurements. Isotope effects were negligible for the ALD chemistry considered next.

HfO_2 growth was carried out in a home-built ALD reactor as shown in Figure 1. Short pulses (10 s) of TEMAH (carried with purified N_2) and pure D_2O vapor were delivered alternately to the ALD chamber through stainless steel tubing with VCR fittings. After each precursor exposure, the ALD chamber was purged for 5 min with purified N_2 and pumped briefly to prevent contamination from gas-phase products and cross-reaction with residual precursor molecules. To reduce oxygen impurities down to 10^{-6} ppm in the N_2 carrier gas of TEMAH, a home-built prefilter and a commercially available N_2 purifier (Centorr Vacuum Industries equipped with an oxygen sensor) were used. The exposure doses and pulse lengths (10 s) were electronically controlled by MKS mass flow controllers and diaphragm valves. During film deposition, the pressure of the reactor chamber was monitored with a Baratron (MKS) and maintained at ~3 Torr by a throttle valve (MKS) located between the reactor chamber and a drag-diaphragm dry pump unit (Alcatel).

(10) See, for instance: http://www.intel.com/technology/silicon/45nm_technology.htm.
(11) Note the pioneering work of George et al. on characterizing the ALD growth: Dillon, A. C.; Ott, A. W.; George, S. M.; Way, J. D. *Surf. Sci.* **1995**, *322*, 230.
(12) Stefanov, B. B.; Gurevich, A. B.; Weldon, M. K.; Raghavachari, K.; Chabal, Y. J. *Phys. Rev. Lett*. **1998**, *81*, 3908.
(13) Kand, S.-W.; Rhee, S.-W. *J. Vac. Sci. Technol., A* **2004**, *22*, 2392.
(14) Kelly, M. J.; Han, J. H.; Musgrave, C. B.; Parsons, G. N. *Chem. Mater.* **2005**, *17*, 5305.
(15) Kern, W.; Puotinen, D. *RCA Rev.* **1970**, *31*, 187.
(16) Chabal, Y. J.; Higashi, G. S.; Raghavachari, K.; Burrows, V. A. *J. Vac. Sci. Technol., A* **1989**, *7*, 2104.
(17) Higashi, G. S.; Becker, R. S.; Chabal, Y. J.; Becker, A. J. *Appl. Phys. Lett.* **1991**, *58*, 1656.
(18) Higashi, G. S.; Chabal, Y. J.; Trucks, G. W.; Raghavachari, K. *Appl. Phys. Lett*. **1990**, *56*, 656.

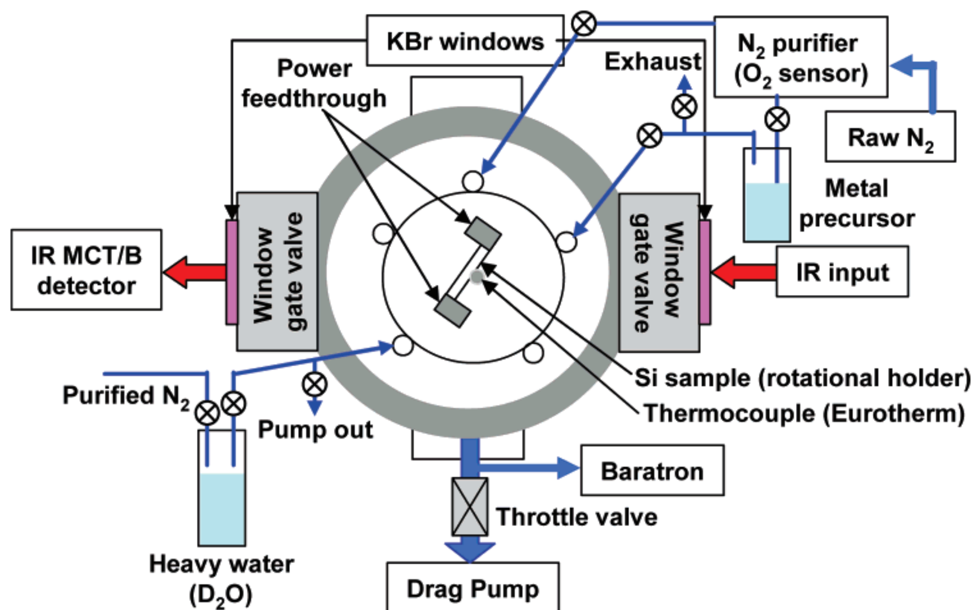

Figure 1. Schematic diagram of the ALD reactor (not to scale) with a transmission IR spectrometer for in situ surface characterization. The KBr windows are protected by gate valves during ALD precursor exposures. During growth, the chamber was maintained at 60 °C.

The samples were mounted on a rotating manipulator with tantalum clips (for direct resistive heating). Samples were heated up to 100 ± 2 °C for film deposition and maintained at 60 ± 0.1 °C for IR data acquisition, as measured with a K-type (chromel−alumel) thermocouple. The chamber walls and all gas lines were maintained at 60 °C throughout the process. To avoid contamination of the KBr windows by TEMAH or D_2O during growth, two gate valves separating the windows from the chamber were closed during each precursor exposure and opened during the purging cycle when data were acquired. To investigate the thermal stability of the ALD-grown films, postannealing was performed immediately after HfO_2 film deposition, either in situ (up to ∼700 °C) in ultra-pure N_2 purge for IR measurements or after an ex situ transfer into a UHV chamber (up to ∼960 °C in a base pressure of $\sim10^{-10}$ Torr) for MEIS measurements.

Thin Film Characterization. In situ surface analysis was performed with a Nicolet Nexus 670 interferometer and a liquid nitrogen cooled MCT/B detector, providing submonolayer sensitivity for most surface chemical species. All IR data were taken in the 400−4000 cm^{-1} spectral range with 4 cm^{-1} resolution. To observe both the transverse and the longitudinal optical (TO and LO) phonon modes of surface chemical species in the spectral region below 1500 cm^{-1}, measurements were performed in single-pass transmission geometry with the IR beam incident at 70° with respect to the surface normal (close to the Brewster angle).

The composition of the ALD-grown HfO_2 films was measured with RBS. The SIMNRA simulation program[19] was used to extract the areal densities of relevant elements from the recorded RBS spectra. The thickness of the HfO_2 layer was estimated using the Hf RBS signal only, assuming that the HfO_2 thin film density was that of bulk HfO_2 (9.69 g/cm^3 or 8.316 × 10^{22} atoms/cm^3). For highly contaminated films with significant carbon concentration (C/Hf atomic ratio ∼1), the real physical thickness can be substantially higher (about twice). To detect elements lighter than the Si substrate (e.g., C and O), the Si RBS signal was suppressed using ion channeling and grazing emission detection (detector positioned at 86° relative to the surface normal).

(19) Mayer, M. SIMNRA, version 4.40; Forschungszentrum Jülich Institute für Plasmaphysik, Jülich, Germany.

MEIS was used to determine the elemental depth distribution of atoms present in multiple layer structures, such as $HfO_2/Si_xN_y/Si$. The MEIS experiments were performed with 130.8 keV H^+ beams using a double alignment geometry in the (110) scattering plane, in which the incoming beam was aligned with the Si[100] channeling direction, and the detector axis was aligned with the [$\bar{1}$11] crystallographic axis. Such scattering geometries were very useful for reducing backscattered background signal from bulk Si and allowed a detailed study of the otherwise weak O signal. Backscattered ion energies were analyzed with a high-energy resolution toroidal electrostatic ion detector ($\Delta E/E = \sim0.1\%$).[20] Depth profiles of the elements were obtained from simulations of the backscattered ion energy distribution (with the assumption that film densities were known or could be extrapolated from films of known composition). Quantitative depth profiles for different species can be extracted with a resolution as high as 3 Å in the near-surface region. However, the depth resolution deteriorates for deeper layers[21] due to the statistical nature of the ion−solid interaction. X-ray photoelectron spectroscopy (XPS) was also used to detect chlorine impurities for HfO_2 deposited on Cl/Si. The atomic structure of the ALD-grown HfO_2 film was characterized with high-resolution transmission electron microscopy (HRTEM). For capacitance ($C-V$) and leakage current ($I-V$) measurements of the high-κ film, an Hg probe of 7.3 × 10^{-4} cm^2 was used for electrical contact.

Results and Discussion

Stability of Prefunctionalized Silicon Surfaces during Initial ALD. A detailed characterization of the starting surfaces prior to ALD growth is crucial for understanding HfO_2 film nucleation. In this section, we first present IR characterization of silicon surfaces passivated with hydrogen (H/Si), chlorine (Cl/Si), an ultra-thin layer of silicon oxides

(20) Tromp, R. M.; Copel, M.; Reuter, M. C.; Horn von Hoegen, M.; Speidell, J.; Koudijs, R. *Rev. Sci. Instrum.* **1991**, *62*, 2679.
(21) Schulte, W. H.; Busch, B. W.; Garfunkel, E.; Gustafsson, T.; Schiwietz, G.; Grande, P. L. *Nucl. Instrum. Methods Phys. Res., Sect. B* **2001**, *16*, 1883.

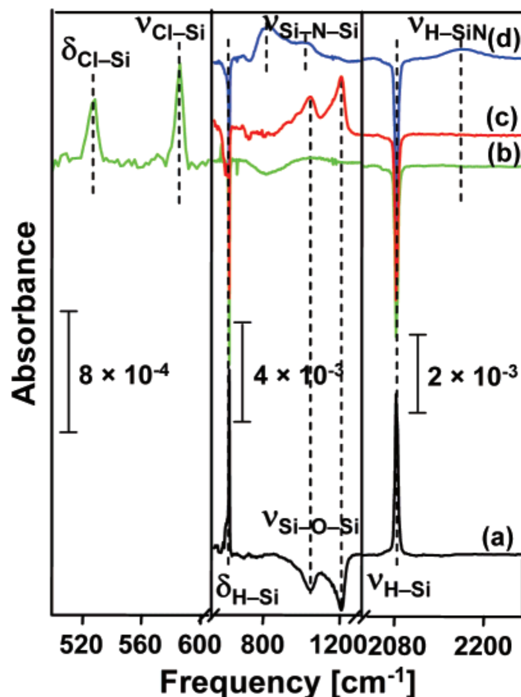

Figure 2. Transmission IR spectra of Si(111) surfaces passivated with (a) hydrogen, (b) chlorine, (c) RCA SiO_2, and (d) silicon nitride. Spectrum a is referenced to an oxidized surface, and spectra b−d are referenced to a fully H-terminated Si(111). All spectra were obtained with the sample at 60 °C, and the IR beam was aligned 70° to the surface normal.

(O/Si), and silicon nitride (Si_xN_y/Si). The ability to prevent silicon oxidation during HfO_2 atomic layer growth is then evaluated for these four surface terminations.

Chemical Nature of Functionalized Surfaces. Figure 2a shows an IR spectrum of atomically flat monohydride-terminated Si(111) surface formed at room temperature by NH_4F etching, referenced to a RCA oxidized surface. The very sharp (resolution limited) bands at 627 and 2083 cm^{-1} are the signatures of Si−H bending and stretching vibrational modes, indicating highly homogeneous surfaces with a low defect density. The two negative broad bands labeled $\nu_{Si-O-Si}$ correspond to the TO and LO phonon of the thin oxide layer on the reference sample. After a Cl_2 gas-phase treatment, hydrogen was completely replaced by chlorine, as evidenced in Figure 2b by the complete removal of the Si−H features and the appearance of two modes at 527 and 586 cm^{-1}, assigned to Si−Cl bending and stretching vibrational modes.[22] The Cl-terminated surface remained atomically flat as evidenced by the narrow width of these two features (full width at half-maximum (fwhm) = ∼6 cm^{-1}). Surfaces of thinly oxidized wafers, prepared by an RCA treatment of initially H-terminated surfaces, were characterized by TO (1048 cm^{-1}) and LO (1210 cm^{-1}) modes of amorphous SiO_2 (∼0.5 nm) as shown in Figure 2c.[23] Finally, the Si_xN_y/Si surfaces generated by thermal nitridation of H/Si(111) at ∼500 °C in pure NH_3 showed two broad features at 840 and 1040 cm^{-1} (TO and LO modes of Si_xN_y, respectively) as shown in Figure 2d.[24] The broadband centered at 2175 cm^{-1} was assigned to the H−SiN_x stretching mode[25] with the N atoms inserted in the Si−Si back-bond, indicating that the nitride surface was terminated by hydrogen. The absence of any SiO_2 and SiO_xN_y phonon modes in Figure 2d indicates that oxygen incorporation in the nitride layer was negligible.

Silicon nitride has been widely used as a gate barrier layer to prevent oxygen and boron migration[1,26] and also protects silicon against water vapor oxidation up to ∼600 °C.[27] The present paper therefore emphasizes HfO_2 growth on nitrided silicon surfaces. To be an effective oxidation barrier during HfO_2 ALD, the nitride layer must be continuous and as thin as possible to minimize the EOT for the high-κ stack. It is therefore important to monitor the silicon nitridation process in situ prior to the HfO_2 growth.

Transmission IR spectra in Figure 3 show the formation of Si_xN_y upon exposing H-terminated Si(111) (Figure 3a) to pure NH_3 gas (∼5 Torr) at different temperatures. Up to 300 °C, there was no loss of the Si−H stretching mode at 2083 cm^{-1} or growth of the Si−N−Si mode at ∼840 cm^{-1} (Figure 3b−d). In these spectra, the oscillation below 1200 cm^{-1} with a periodicity of ∼200 cm^{-1} is due to an interference resulting from slight variations in the Si substrate temperature. At 400 °C (Figure 3e), the Si−H stretching mode intensity was reduced by ∼15% and its frequency red-shifted (∼4 cm^{-1}). This observation is more consistent with the reaction of NH_3 with defect sites, such as steps and triangular pits typically found on H/Si(111) surfaces, rather than direct reaction with flat H-terminated surfaces. The feature at 1535 cm^{-1} was assigned to the SiN−H_2 bending mode,[28] suggesting that reactions at such sites involve NH_3 dissociation without N incorporation into the Si−Si network. However, the appearance of the SiN−H_2 species (particularly at higher temperature processing) should be interpreted cautiously because the appearance depends on the conditions of NH_3 exposure. For instance, SiN−H_2 species were not observed in a previous study[27] when a gas mixture of 4% NH_3 in N_2 was used instead of pure NH_3. We also find that, if we purged the reactor with N_2 after the NH_3 treatment, fewer SiN−H_2 species were observed. These observations indicate that the formation of surface NH_2 can also occur after the surface was nitrided by NH_3 dissociation on Si_xN_y. While it is well-known that NH_3 chemisorbs on clean Si-(100)-(2 × 1),[29] the situation on nitrided (or even H-terminated) surfaces is not well-understood and is now being investigated in detail on a variety of well-defined partially nitrided and H-terminated Si surfaces in our lab.

Upon NH_3 exposure of H/Si(111) at 500 °C (Figure 3f), the sharp Si−H stretching mode at 2083 cm^{-1} was dramatically broadened and blue-shifted (to 2175 cm^{-1}), suggesting

(22) Rivillon, S.; Amy, F.; Chabal, Y. J.; Frank, M. M. *Appl. Phys. Lett.* **2004**, *85*, 2583.
(23) Chabal, Y. J. *Fundamental Aspects of Silicon Oxide*; Springer-Verlag: Berlin, 2001.
(24) Semmache, B.; Lemiti, M.; Chaneliére, C.; Dubois, C.; Sibai, A.; Canut, B.; Laugier, A. *Thin Solid Films* **1997**, *296*, 32.
(25) Lin, K.-C.; Lee, S.-C. *J. Appl. Phys.* **1992**, *72*, 5474.
(26) Takeuchi, H.; King, T. J. *Appl. Phys. Lett.* **2003**, *83*, 788.
(27) Brewer, R. T.; Ho, M.-T.; Zhang, K. Z.; Goncharova, L. V.; Starodub, D. G.; Gustafsson, T.; Chabal, Y. J. *Appl. Phys. Lett.* **2004**, *85*, 1.
(28) Klaus, J. W.; Ott, A. W.; Dillon, A. C.; George, S. M. *Surf. Sci.* **1998**, *418*, 14.
(29) Queeney, K. T.; Chabal, Y. J.; Raghavachari, K. *Phys. Rev. Lett.* **2001**, *86*, 1046.

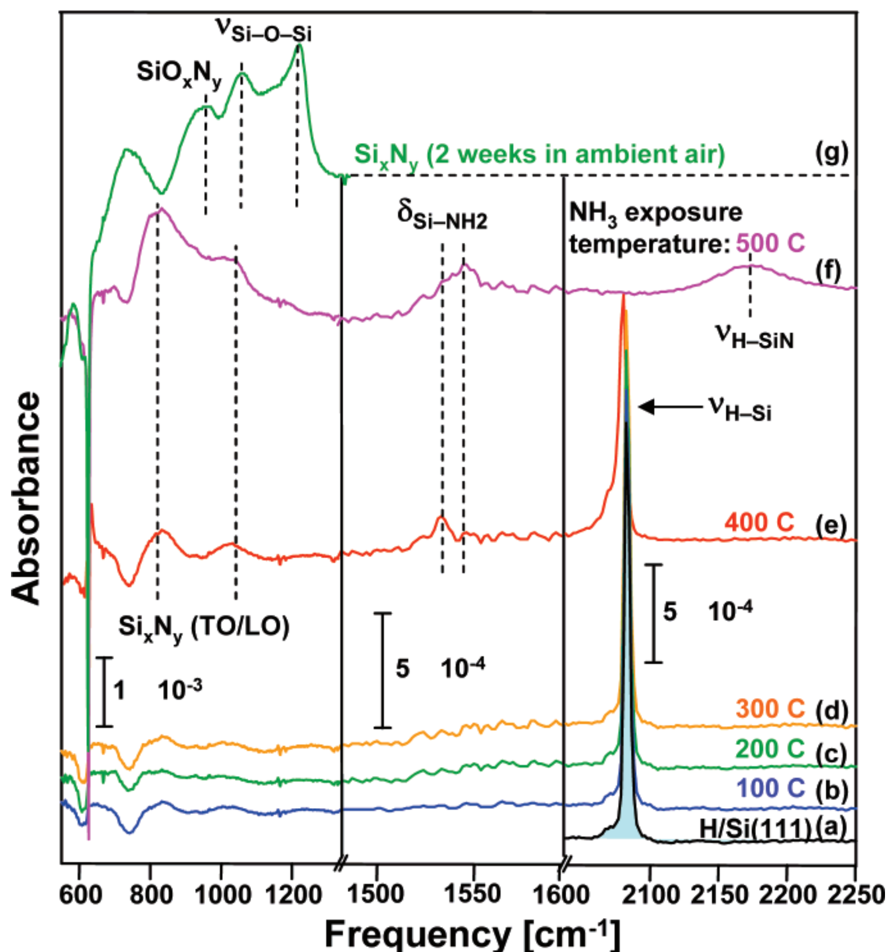

Figure 3. Transmission IR spectra showing the reactivity of H/Si(111) to pure NH_3 gas (~5 Torr) at different temperatures: (a) H/Si(111) prior to NH_3 exposure and (b−f) after NH_3 exposure from 100 to 500 °C. Spectrum g is that of silicon nitride (formed by previous procedures) after 2 week exposure to ambient air. The reference surfaces are oxidized silicon for the high-frequency region (2050−2250 cm^{-1}) and H/Si(111) for the low-frequency region (600−1600 cm^{-1}).

the insertion of N into Si−Si back-bonds.[30,31] The SiN−H_2 bending mode also broadened and exhibited a large blue-shift. At the same time, both TO and LO Si_xN_y phonon modes were observed at 840 and 1040 cm^{-1}, indicating that a continuous layer of silicon nitride formed at 500 °C. In contrast to the situation at 400 °C when NH_2 could be formed directly at defect sites, the flat H-terminated terrace sites can now be attacked, with insertion of N into the Si−Si bonds. At 500 °C and higher processing temperatures, the observation of NH_2 is most likely associated with NH_3 reaction with the nitrided surface during cool down in NH_3, accounting for the blue-shift and larger width of the Si−NH_2 mode.

The thickness of the Si_xN_y layer formed at 500 °C is ~5 Å as measured by MEIS (described later), which effectively protects silicon from being oxidized by the ALD oxidant D_2O up to 600 °C.[27] However, the same nitride layer does not prevent slow oxidation in air. For instance, Figure 3g shows that, after 2 weeks in ambient air, an interfacial SiO_2 layer was formed and that the original silicon nitride was oxidized into oxynitride (TO mode at 968 cm^{-1}).[32] The instability of Si_xN_y in air suggests that nitridation should be performed in situ prior to ALD film deposition to minimize the oxygen concentration in the nitride layer.

ALD Growth of HfO_2. ALD-grown HfO_2 on prefunctionalized Si substrates was first characterized with RBS by focusing on the Hf concentration. The film thickness was calculated from the areal density of the Hf peak with ±6% uncertainty. Figure 4a,b presents the RBS spectra of HfO_2 (20 ALD cycles) on silicon taken at a backscattering angle of 20° from the surface normal both in random and in channeling geometries. Channeling helps suppress the signal from the Si substrate. To improve RBS sensitivity to low mass elements (lighter than the Si substrate), grazing angle detection (86° relative to the surface normal) was used in combination with channeling. In this case, light elements, such as C and O, can be quantified (Figure 4c). The measured atomic concentrations (see Figure 4 caption) correspond to 2.48 nm HfO_2 and 1.93 nm SiO_2. The relatively large coverage of C atoms (10^{16} C atoms/cm^2) arises from hydrocarbon contamination of the surface (during transfer) and possibly hydrocarbons inside the film.

Figure 5 shows the RBS-derived hafnium oxide film thickness on H/Si, Cl/Si, O/Si, and Si_xN_y/Si surfaces. Linear growth of HfO_2 was observed on SiO_2 passivated silicon from the first ALD cycle with a deposition rate of ~0.11 nm/cycle. A slightly lower growth rate, but still linear, was

(30) Holt, J. K.; Goodwin, D. G.; Gabor, A. M.; Jiang, F; Stavola, M.; Atwater, H. A. *Thin Solid Films* **2003**, *430*, 37.
(31) Kakiuchia, H.; Nakahamab, Y.; Ohmia, H.; Yasutakea, K.; Yoshiia, K.; Mori, Y. *Thin Solid Films* **2005**, *479*, 17.
(32) Ay, F.; Aydinli, A. *Opt. Mater.* **2004**, *26*, 33.

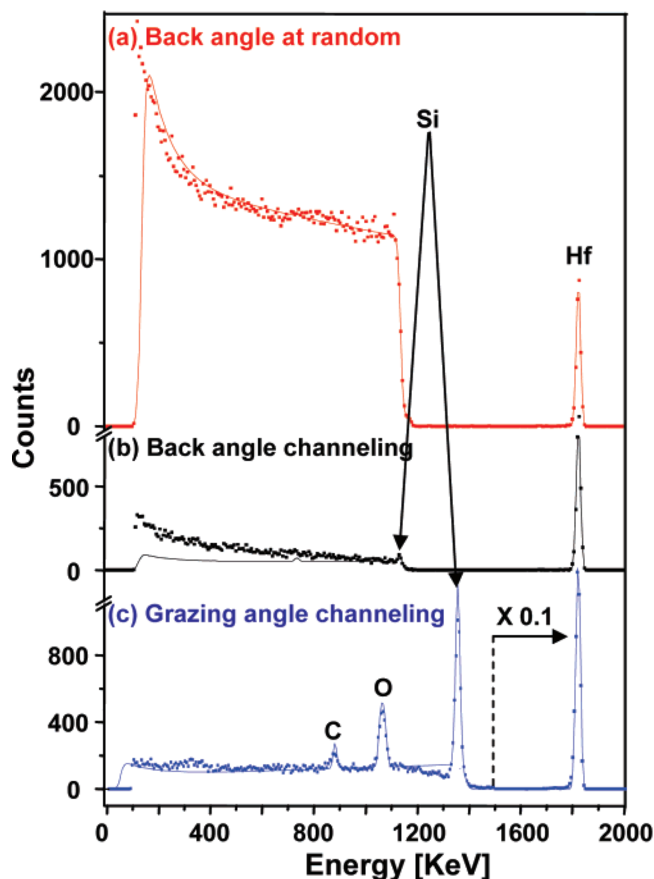

Figure 4. RBS data using geometry to enhance the detection of Hf and other light elements with two detectors placed at a back angle and a grazing angle (20 and 86° to the surface normal, respectively) with incidence optimized for channeling. The dots and solid lines represent experimental and simulated data, respectively. (a) Back angle spectrum provides Hf content: 6.88×10^{15} Hf atoms/cm^2. (b) Back angle channeling spectrum provides improved sensitivity to low mass elements (Si RBS signal reduction), but C and O cannot be detected. (c) Grazing angle detector combined with channeling provides the best sensitivity for low mass elements: C about 10^{16} atoms/cm^2 and O about 22.5×10^{15} atoms/cm^2.

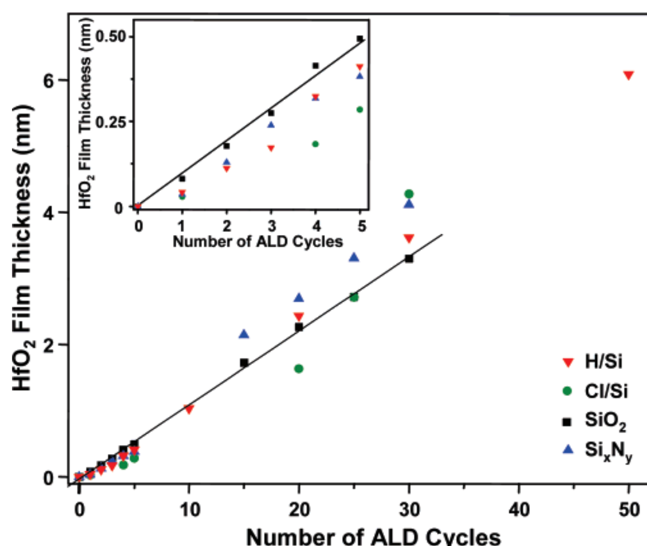

Figure 5. HfO_2 thickness, estimated from RBS measurements (~12% uncertainty) of ALD-grown HfO_2 as a function of deposition cycles for growth on H/Si, Cl/Si, RCA SiO_2, and silicon nitride. The inset highlights the HfO_2 growth during the first five ALD cycles.

observed on H/Si and Si_xN_y/Si surfaces during the first 5 ALD cycles (see inset of Figure 5), suggesting that HfO_2

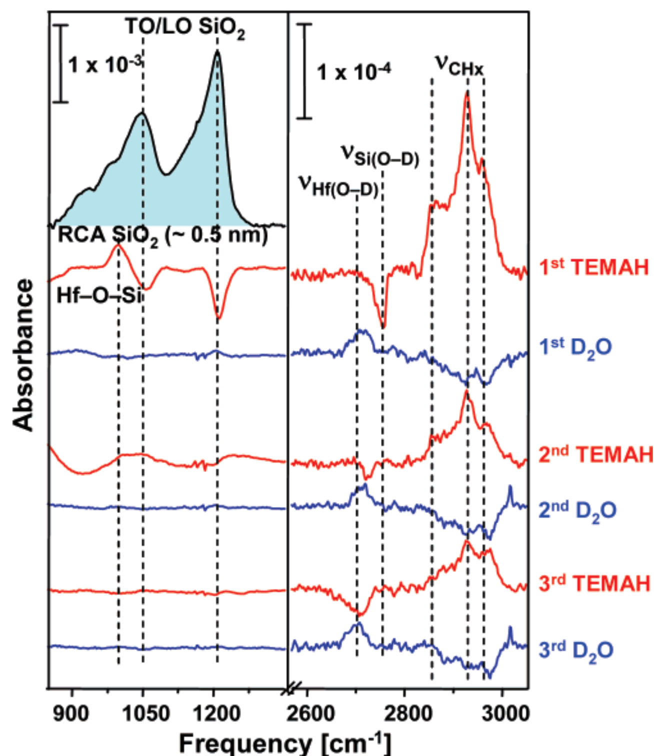

Figure 6. Transmission IR spectra showing the interaction of TEMAH and D_2O with RCA SiO_2 passivated silicon after each precursor exposure. All spectra were referenced to the surface prior to the last reaction cycle. The two spectral regions show the alternate presence of OD and CH_x surface species and the interfacial structure of Hf−O−Si formed in the early stages of film nucleation.

nucleation is favorable on these surfaces. In contrast, nonlinear growth was observed for Cl-terminated surfaces, indicating that there exists a larger nucleation barrier. The lower reactivity of Cl−Si toward the TEMAH precursor may be due to the higher bond energy of Si−Cl (~381 kJ/mol) than the Si−H, NH_x, or OH bond energies.

The stability of these four starting surfaces in water vapor was previously studied: H/Si,[33] Cl/Si,[34] Si_xN_y/Si,[27] and O/Si are all stable in water vapor at ~100 °C in an oxygen-free environment. Therefore, differences in the initial growth of HfO_2 likely arise from other factors. In the next section, we present a detailed investigation of the surface reactions during the layer-by-layer growth of HfO_2 on silicon combining in situ and ex situ surface characterization techniques.

Interface Reactions during HfO_2 Growth on Prefunctionalized Silicon. Understanding how surface prefunctionalization affects film nucleation, composition, and structure is best investigated with in situ IR characterization by examining the changes of surface chemical species occurring during HfO_2 ALD. For example, in situ IR spectroscopy can quantify the concentration of hydroxyl groups on oxidized Si surfaces, which have been shown to affect the initial HfO_2 growth rate,[35] and give insights into the initial TEMAH interaction with SiO_2.

(33) Frank, M. M.; Chabal, Y. J.; Wilk, G. D. *Appl. Phys. Lett*. **2003**, *82*, 4758.
(34) Rivillon, S.; Brewer, R. T.; Chabal, Y. J. *Appl. Phys. Lett*. **2005**, *87*, 1.
(35) Green, M. L.; Ho, M.-Y.; Busch, B.; Wilk, G. D.; Sorsch, T.; Conard, T.; Brijs, B.; Vandervorst, W.; Ràisànen, P. I.; Muller, D.; Bude, M.; Grazul, J. *J. Appl. Phys.* **2002**, *92*, 7168.

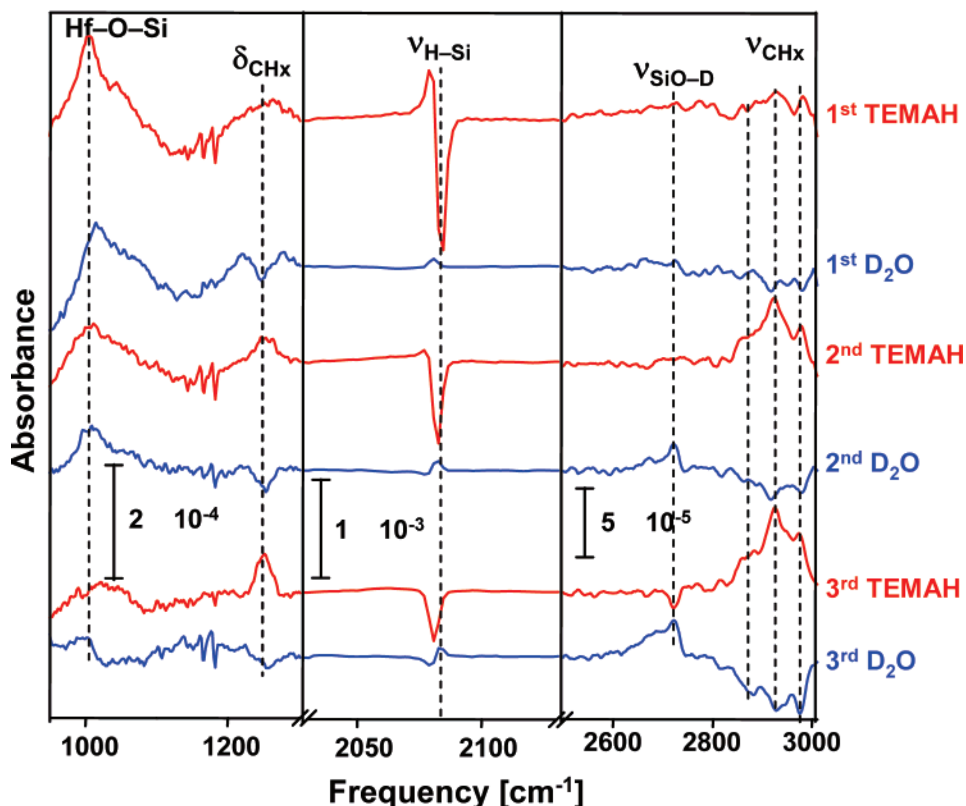

Figure 7. Transmission IR spectra showing the interaction of TEMAH and D_2O with H/Si(111) after each precursor exposure. All spectra are referenced to the surface prior to the last reaction cycle. Three spectral regions showing the formation of interfacial Hf–O–Si, the Si–H stretching vibration, and the alternate presence of OD and CH_x species.

Oxide-Terminated Surfaces. Figure 6 summarizes the chemical evolution of the surface after each half ALD cycle on SiO_2-terminated surfaces (i.e., each spectrum is referenced to that of the surface right before the last half cycle). For these oxidized surfaces, initially terminated by OD groups, TEMAH first reacted with these groups as shown by a loss of Si–OD (negative band at 2750 cm^{-1}) and a gain of CH_x groups (positive bands in the spectral region 2800–3000 cm^{-1}). Second, chemisorption of the Hf precursor to the SiO_2-passivated surface altered the Si–O–Si arrangement of the very top SiO_2 layer enough to produce a loss of intensity in the SiO_2 phonon mode region (1020–1250 cm^{-1}). Third, a feature centered at 1000 cm^{-1} was clearly observed after the first TEMAH exposure, assigned to Hf–O–Si bonds. It is evidence for direct chemical bonding between HfO_2 and SiO_2.[36] The absence of this feature in the following difference spectra confirms that, in contrast to growth on the H-terminated Si surface,[37] a saturated coverage was achieved after the first TEMAH cycle (i.e., additional Hf–O–Si bonds are not formed during the subsequent reactions).

During the subsequent precursor exposures, the alternating loss and gain of CH_x and Si–OD absorption bands (Figure 6) indicated that a ligand exchange reaction took place. However, the strength of the two bands was slightly different for loss and gain, indicating an incomplete ligand exchange. As a result, it was expected that some CH_x and OD groups may accumulate in the ALD-grown film. Also, the intensity gain of the CH_x groups on the surface was larger after the first TEMAH exposure than for after the subsequent TEMAH exposures. These observations suggest that TEMAH reacts more completely with Si–OD than with Hf–OD. The low-frequency region of the spectra in Figure 6 shows no increase of the SiO_2 phonon intensity, indicating that no additional SiO_2 was formed during the early stages of HfO_2 film deposition.

Hydrogen-Terminated Surfaces. Figure 7 displays IR difference spectra for HfO_2 growth on H/Si. For the first TEMAH exposure, there was a loss of Si–H accompanied by a gain of CH_x, indicating that a reaction occurred between the Hf precursor and the H/Si surface. However, the CH_x stretch mode intensity was much lower than for the first TEMAH pulse on the SiO_2 surfaces. For subsequent cycles, the ligand exchange reaction was similar to what was observed for SiO_2 surfaces, consistent with the growth rates measured by RBS (Figure 5). The appearance of Hf–O–Si at ~1000 cm^{-1} right after the first TEMAH pulse (i.e., prior to any D_2O pulse) suggests that D_2O cannot be fully eliminated in the reactor, resulting in some hydrolyzation of TEMAH [e.g., HO–Hf–$(NCH_3C_2H_5)_3$] or a possible reaction of D_2O with the surface after TEMAH adsorption.[38] It also points out that oxygen incorporation into Si–Hf bonds is energetically highly favorable.

(36) Cosnier, V.; Olivier, M.; Théret, G.; André, B. *J. Vac. Sci. Technol., A* **2001**, *19*, 267.
(37) Ho, M.-T.; Wang, Y.; Brewer, R. T.; Wielunski, L. S.; Chabal, Y. J.; Moumen, N.; Boleslawski, M. *Appl. Phys. Lett.* **2005**, *87*, 133103.
(38) Fenno, R. D.; Halls, M. D.; Raghavachari, K. *J. Phys. Chem. B* **2005**, *109*, 4969.

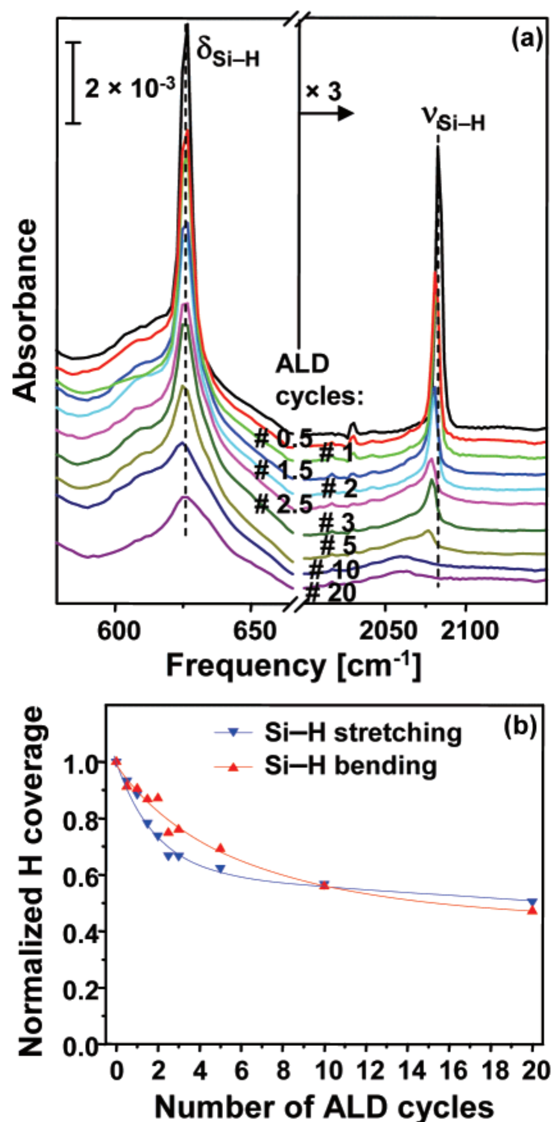

Figure 8. (a) Transmission IR spectra of a fully H-passivated Si(111) surface (top spectrum) and a H/Si(111) surface after a specific number of TEMAH and D_2O exposures in the Si−H stretching and bending mode regions. All spectra are referenced to an oxidized surface. (b) Normalized surface hydrogen coverage (approximately ±5% uncertainty) after TEMAH and D_2O exposures; the ratio is calculated from the integration of Si−H stretching and bending mode intensity after a specific number of ALD cycles.

Figure 8a shows that the loss of Si−H occurs during TEMAH exposures (0.5, 1.5, and 2.5 cycles) rather than upon D_2O exposure (1 and 2 cycles). Steric interactions limit the reaction to only ∼50% of the surface sites as evidenced in Figure 8b: half of the initial Si−H stretching intensity remains after the interface has stabilized (5−10 cycles). Once stabilized, the interface was characterized by red-shifted Si−H stretching and broadened Si−H bending modes, due to the close proximity of the Si−O−Hf neighbors.

The linear increase of Hf coverage (Figure 5) indicates that the total amount of Hf atoms deposited per cycle remained constant, typical of a layer-by-layer growth. Yet, the IR data showed that 5−10 cycles were needed for the interface to stabilize (with only 50% of the surface reacted at the end). This observation is in contradiction with a layer-by-layer growth for the first 10 cycles. Instead, taken together, the RBS and IR data suggested that Hf was deposited into more than just one layer per cycle during the initial growth. While the Hf amount deposited remained the same on average, its distribution was not perfectly two-dimensional for each cycle, particularly during the first 1−3 cycles.

Chlorine-Terminated Surfaces. Figure 9a summarizes the results of HfO_2 film nucleation on Cl/Si(111). The behavior of the Si−Cl modes is similar to that of Si−H modes on H/Si. There is no loss of Si−Cl bending and stretching mode intensity upon D_2O exposures for all cycles but clear reaction with TEMAH. There is also no formation of interfacial SiO_2 (not shown). Therefore, it appears that Cl-terminated surfaces remain as stable as H-terminated surfaces during growth. In particular, it takes 5−10 cycles for the interface to reach its stable configuration with ∼50% unreacted Si−Cl sites. The Hf coverage incubation period observed with RBS (Figure 5) is consistent with this observation. RBS is also helpful to determine whether chlorine remains after growth. There is some debate in the literature as to whether the presence of chlorine can generate electronic and structural defects in the high-κ layer in the $HfCl_4$-generated HfO_2.[39,40] Figure 10 shows that the Cl atomic density is $\sim 1.2 \times 10^{14}$ atoms/cm^2 in the as-grown HfO_2 film. This Cl residue corresponds to ∼15% of the surface atomic density of a Si(111) plane.

Nitride-Terminated Surfaces. Figure 11 shows the IR absorbance spectra of HfO_2 grown on a thin Si_xN_y passivated silicon substrate (∼5 Å Si_xN_y obtained by 500 °C anneal in NH_3 for 2 min), referenced to the starting nitrided surface. The bottom four spectra (right panel) show ligand exchange with a steady increase of both OD and CH_x in the film, as was observed for H/Si, Cl/Si, and O/Si surfaces. As expected, there is no interfacial SiO_2 observed during film deposition on Si_xN_y/Si. The weak broad bands centered at 890 and 1125 cm^{-1} are assigned to phonon modes associated with the silicon nitride/HfO_2 interface (Hf−O−Si_xN_y). The intensity dependence of these interfacial Si−O−Hf modes is faster than that observed on other surfaces (bottom left inset), indicating that only ∼3−5 cycles are needed to reach the steady state interfacial configuration. After 20 cycles (∼2 nm HfO_2 film), the HfO_2 TO and LO phonon modes are observed at 540 and 680 cm^{-1}, respectively, with an intensity consistent with the RBS determined coverage of Hf (Figure 5).

The MEIS spectrum (Figure 12a) makes it possible to quantify the concentrations and depth profiles of Hf, O, N, and C on the Si substrate. The thickness of HfO_2 (∼2.1 nm after 20 ALD cycles) and interfacial nitride layer (∼0.50 nm) was extracted by measuring the concentration of Hf, O, and N atoms and assuming the density of bulk HfO_2 and stoichiometric Si_3N_4. The best correlation between calculated and experimental ion yield was obtained by assuming excess oxygen in the Hf oxide layer with an average stoichiometry

(39) Liu, D. R.; Roan, D.; Ramon, M.; Edwards, N. V.; Gregory, R.; Werho, D.; Kulik, J.; Tam, G.; Irwin, E.; Wang, X. D.; La, L. B.; Hobbs, C.; Garcia, R.; Baker, J.; White, B. E.; Tobin, P. *J. Electrochem. Soc.* **2004**, *151*, 220.

(40) Delabie, A.; Caymax, M.; Brijs, B.; Brunco, D. P.; Conard, T.; Sleeckx, E.; Van Elshocht, S.; Ragnarsson, L.-Å.; De Gendt, S.; Heyns, M. M. *J. Electrochem. Soc.* **2006**, *153*, 180.

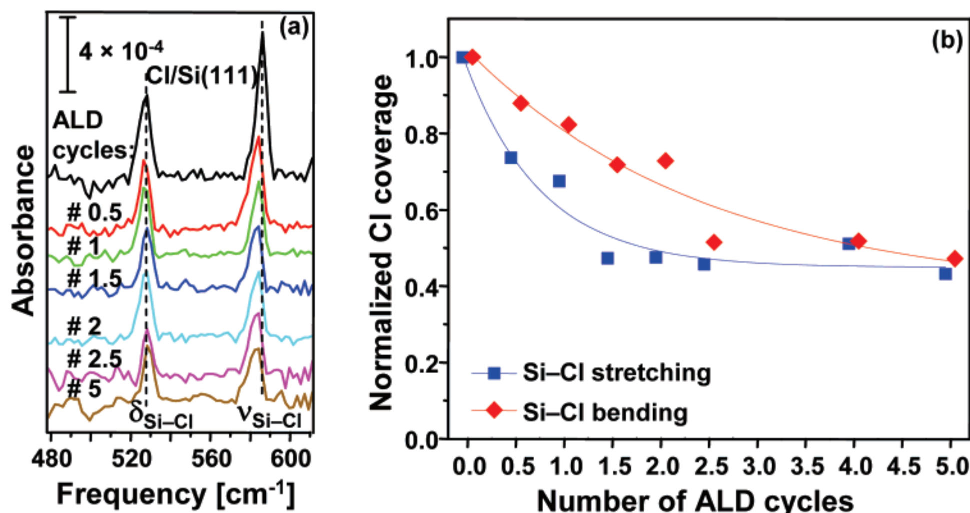

Figure 9. (a) Transmission IR spectra of a fully chlorinated Si(111) surface (top spectrum) and surfaces after a specific number of TEMAH and D_2O exposures in the Si−Cl stretching and bending mode regions. All spectra are referenced to a fully H-terminated surface. (b) Normalized surface chlorine coverage (approximately ±8% uncertainty) after TEMAH and D_2O exposures; the ratio is calculated from the integration of Si−Cl stretching and bending mode intensity after a specific number of ALD cycles.

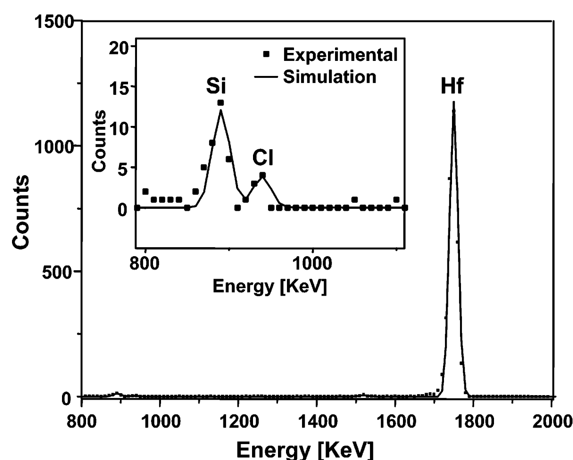

Figure 10. RBS spectrum showing HfO_2 (∼0.2 nm) deposited on Cl/Si. The inset shows Cl residues in the HfO_2/Si stack corresponding to 1.2 × 10^{14} Cl atoms/cm^2. The sample is measured with the back angle detector (20° to surface normal) at a channeling geometry.

of $HfO_{2.2}$. Carbon contamination (1.5 × 10^{15} atoms/cm^2) was detected in the topmost surface layer. Most of the carbon was located at the surface and not in the bulk of the film as determined from its energy position. It was therefore likely due to contaminants arising from the in-air transport from the ALD reactor to the MEIS chamber, a conclusion that is also supported by the fact that it was so easily removed by annealing (reduced to $<0.5 \times 10^{15}$ atoms/cm^2 after annealing). Considering the IR measurements of the HfO_2 films (Figure 11), the extra oxygen atoms may come from OD impurities in the film. The depth profiles of different elements in the MEIS spectrum in Figure 12b suggest a sharp interface in the HfO_2/Si_xN_y/Si stack without detectable Hf diffusion to the interfacial nitride layer.

Electrical Properties. A rough assessment of the role of prefunctionalization on the electrical properties of thin HfO_2 films (∼2 nm) was obtained by looking at preliminary $C-V$ and $I-V$ data for H/Si, Cl/Si, O/Si, and Si_xN_y/Si (Figure 13). For these data, Si(100) was used to better relate to technologically relevant substrates since similar ALD growth studies on H−, Cl−, and nitrided Si (100) surfaces gave

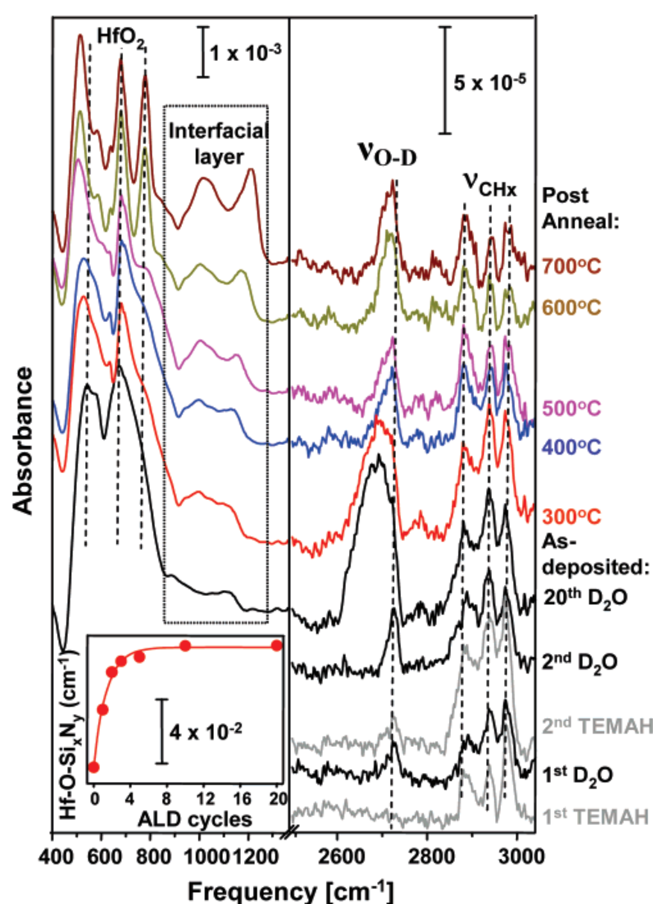

Figure 11. Transmission IR spectra of HfO_2 deposition on ultra-thin silicon nitride and of the film after postannealing in purified N_2 (O_2 < 10^{-6} ppm). All absorbance spectra were referenced to the ALD starting surface (e.g., Si_xN_y passivated silicon formed by thermal nitridation (2 min NH_3 exposure at 500 °C). The inset shows the integrated peak area (∼15% uncertainty) of Hf−O−Si_xN_y phonon modes (860−1200 cm^{-1}) of the as-deposited films, showing that the interfacial layer thickness saturates after approximately five ALD cycles.

results similar to what has been described for Si(111) surfaces. In Figure 13, the data for each run were plotted (typically three samples for each measurement) to emphasize the relatively poor reproducibility from sample to sample.

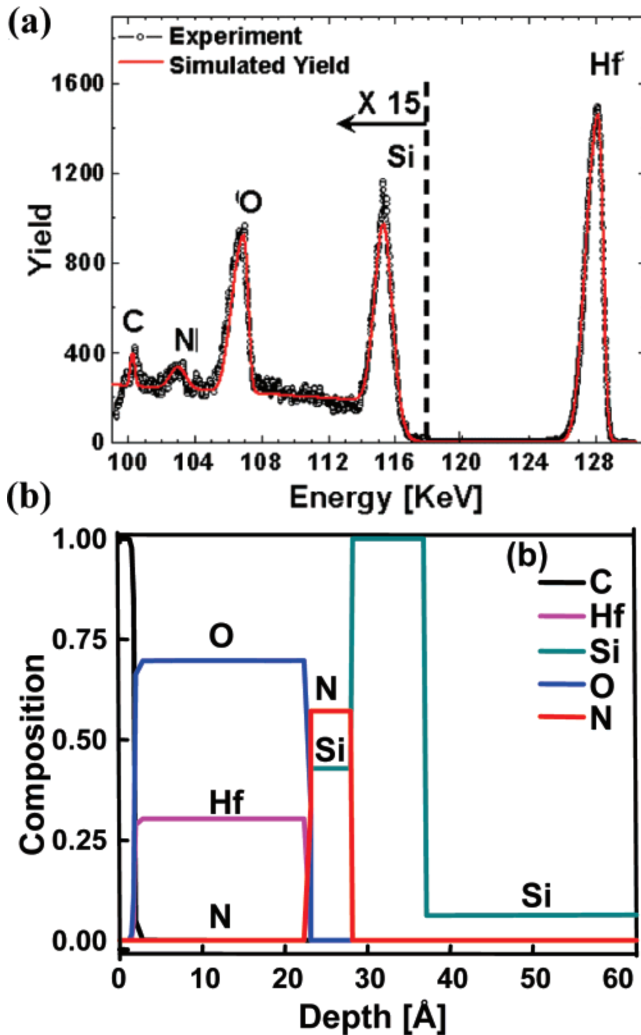

Figure 12. (a) MEIS spectrum of HfO_2 grown on Si_xN_y passivated Si. The nitride was formed by exposing H-terminated silicon surfaces to pure NH_3 at 500 °C. (b) Depth distribution of different elements in the HfO_2 film characterized by spectrum a.

Nonetheless, the sharp slope and the smooth curvature of the $C-V$ data (Figure 13a) suggest that as-deposited HfO_2 films on H/Si(100) have a relatively low interface defect density for the three differently functionalized surfaces. Figure 13b shows that, on average, the leakage level was $\sim 10^{-2}$ A/cm^2 before breakdown. However, poor reproducibility from one measurement to another made it difficult to assess the dependence of the $I-V$ data on the chemical nature of the starting surface.

In summary, the reactivity of the four starting surfaces discussed previously to the TEMAH precursor (determined from the measured IR absorbance intensity of CH_x and Si−OD stretching modes after the first ALD precursor exposure) follows the order: O/Si > Si_xN_y/Si > H/Si > Cl/Si. The interface requires 1, 5, 10, and 10 deposition cycles to reach an equilibrium concentration on SiO_x-, Si_xN_y-, H-, and Cl-passivated surfaces, respectively. At growth temperatures (∼100 °C), there is no formation of interfacial SiO_2. An interfacial layer can be formed upon annealing as discussed in the following section.

Effect of Postdeposition Annealing and Film Contamination. On H/Si, postdeposition annealing of HfO_2/H/Si stacks above 300 °C in purified N_2 removes hydrocarbon absorption and above 500 °C results in interfacial SiO_2 formation and crystallization of the initially amorphous HfO_2 film.[37] In comparison, an ultra-thin nitride layer delays crystallization and minimizes interfacial SiO_2 formation after postannealing.

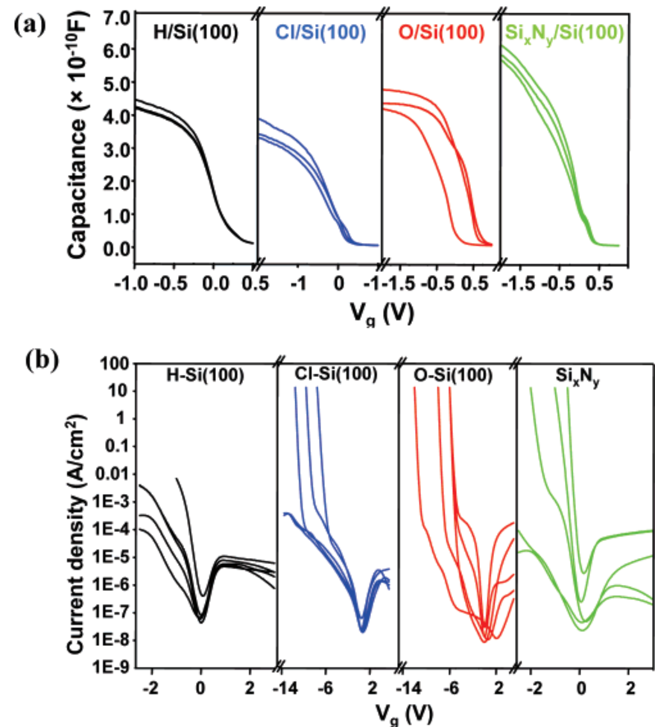

Figure 13. (a) $C-V$ plots for the as-deposited HfO_2 (∼2 nm) grown on hydrogen-, chlorine-, RCA SiO_2-, and Si_xN_y-passivated Si(100) (Si_xN_y formed by 500 °C NH_3 processing). The Hg gate size was 7.3×10^{-4} cm^2. (b) $I-V$ plots for HfO_2 (∼2 nm) deposited on hydrogen-, chlorine-, RCA SiO_2-, and Si_xN_y-passivated Si(100) (Si_xN_y formed by 500 °C NH_3 processing). The Hg gate size was 7.3×10^{-4} cm^2.

Stability of HfO_2 on Si_xN_y. The as-deposited HfO_2 film (∼2.2 nm thick) on Si_xN_y did not crystallize until heated to 600 °C (Figure 11) as opposed to 500 °C for HfO_2 grown on H/Si. Evidence for crystallization was the strong absorbance at 780 cm^{-1} (estimated for the monoclinic HfO_2 LO phonon mode)[41] and the sharpening and red-shift (to 515 cm^{-1}) of the HfO_2 TO mode (Figure 11). The phase transformation of HfO_2 on H/Si upon postannealing in nitrogen is seen in HRTEM images of as-deposited and annealed films (Figure 14a). Similar studies of postannealed HfO_2/Si_xN_y/Si films confirmed that nitrogen stabilizes ALD-grown amorphous HfO_2 by ∼100 °C (not shown).

We have also studied the stability of ALD-grown HfO_2 in ultra-high vacuum (UHV) at higher temperatures with ex situ MEIS. Figure 14b shows that a 2.1 nm thick HfO_2 film densifies at 800 °C, as evidenced by a decrease of the Hf peak width. Complete film decomposition was observed at ∼960 °C, when the O peak completely disappeared, and only Hf and Si surface peaks were observed. Wide shoulders on the low-energy side of the Hf and Si peaks suggest the formation of Hf silicide islands ($HfSi_x$) penetrating deeper into the Si bulk.

Nature of the Interfacial Layer on Si_xN_y. The interfacial structure of HfO_2/Si_xN_y/Si was also strongly affected by

(41) Zhao, X.; Vanderbilt, D. *Phys. Rev. B* **2002**, *65*, 233106.

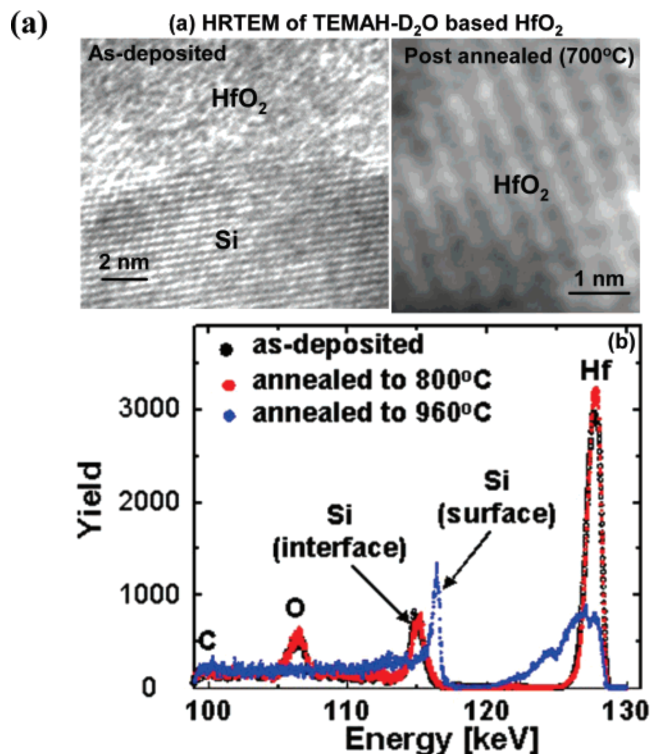

Figure 14. (a) HRTEM images of HfO_2 film (~5.5 nm) deposited on H-terminated silicon before and after postannealing at ~700 °C. (b) MEIS spectra showing HfO_2 film densification grown on H/Si after ex situ postannealing in UHV at ~800 °C. The as-deposited film fully decomposed and formed $HfSi_x$ islands after ~960 °C annealing.

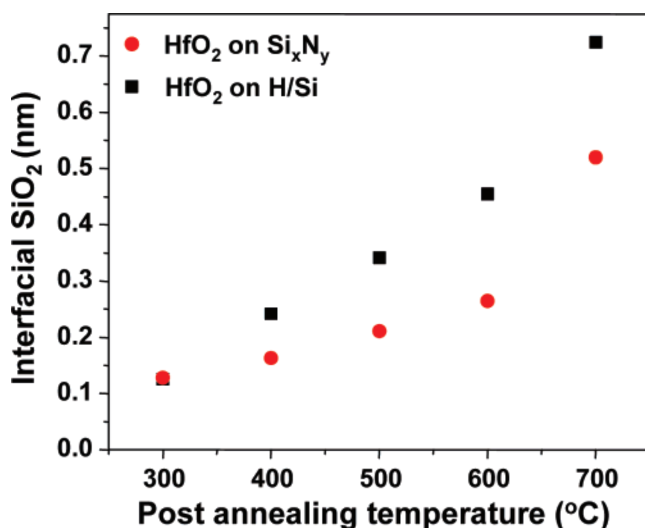

Figure 15. Formation of interfacial silicon oxide during postdeposition annealing of HfO_2 grown on H/Si and Si_xN_y/Si. The SiO_2 thickness (~10% uncertainty), calculated from the integration of SiO_2 TO and LO modes, increased with postannealing temperature.

postdeposition annealing. Figure 11 shows that for a thin Si_xN_y film (~5 Å), there is about the equivalent of one interfacial SiO_2 monolayer (1020−1250 cm^{-1}) formed upon 600 °C postannealing. However, as shown in Figure 15, this is less than observed on H/Si over a wide range of temperatures. If Si substrate oxidation is due to oxygen diffusion into the interface (e.g., from OH or O),[42] we may

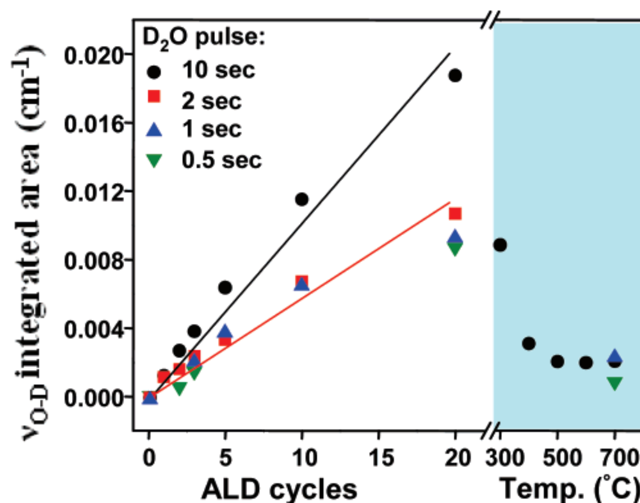

Figure 16. Integrated intensity of O−D stretching mode (~8% uncertainty) in ALD-grown HfO_2 on H/Si as a function of cycles and upon postdeposition annealing.

conclude that even a very thin nitride layer retards oxygen diffusion and minimizes silicon oxidation.

Effect on Electrical Properties. Preliminary data show that postdeposition annealing above 500 °C significantly degrades the capacitance and increased the leakage current (not shown). The crystallization of ALD-grown HfO_2 after high-temperature annealing might be responsible for this electrical property degradation.

Effect on Oxide Film Contaminants. Hydroxyl (i.e., OD in our case) and hydrocarbon contaminants were clearly identified in the as-deposited HfO_2 film regardless of the initial surface chemical functionalization. This can be seen in Figure 11 (right column), where broad bands at ~2650 cm^{-1} (O−D stretch) and in the 2850-3000 cm^{-1} range (CH_x groups) are clearly present after 20 cycles of ALD-grown HfO_2 on Si_xN_y/Si. In general, the quantity of OD and CH_x increased with the number of ALD cycles and with the pulse length of the precursor doses. For instance, Figure 16 shows how the amount of OD groups increases with D_2O pulse length, especially when the pulse length is longer than 2 s. The amount of OD groups also increased linearly with HfO_2 film thickness and decreased dramatically during postannealing. The concentration of hydrocarbons was also decreased by postannealing with more than half of the CH_x removed after 400 °C postannealing. For both hydroxyl and hydrocarbons, disappearance of the IR absorbance bands indicated that these species react, with a loss of hydrogen. Thus, oxygen and carbon most likely remained incorporated in the film or migrated to a nearby interface.

Conclusion

Using TEMAH and D_2O as precursors, the ALD growth of HfO_2 was studied for several prefunctionalized silicon surfaces. In the case of oxide-free surfaces, the growth was initiated primarily by TEMAH, often partially hydroxylated. H/Si, Cl/Si, and Si_xN_y/Si surfaces were all stable to water vapor under typical ALD growth conditions. Hydroxyl groups (OD in our case) were incorporated in the HfO_2 film during growth using water as the oxygen precursor, but there was no formation of interfacial SiO_2 on H/Si, Cl/Si, and

(42) Foster, A. S.; Shluger, A. L.; Nieminen, R. M. *Phys. Rev. Lett*. **2002**, *89*, 225901.

Si_xN_y/Si at the growth conditions. These hydroxyl species led to excess oxygen (forming $HfO_{2.2}$ films).

Linear growth on the hydroxylated SiO_2 surface was observed in both RBS and IR spectra from the very beginning of the film nucleation with a deposition rate of ~0.11 nm per ALD cycle. For H/Si and Si_xN_y surfaces, several cycles were required for the interface to reach its equilibrium composition, although the Hf coverage increased linearly. This apparent contradiction suggests that Hf was not necessarily deposited within a two-dimensional layer (in a perfect layer-per-layer growth mode) during the early cycles but involved instead a rougher growth mode on the microscopic scale initially. For Cl/Si surfaces, both RBS and IR showed an incubation period. The relative reactivity to TEMAH for these surface functionalizations was O/Si > Si_xN_y/Si > H/Si > Cl/Si.

The effect of postannealing on HfO_2 film composition and HfO_2/Si interfacial structure clearly showed that SiO_2 began to develop at the interface as the annealing temperature was raised to 500 °C for H-passivation and 600 °C for nitride passivation. On the other hand, postdeposition annealing effectively removed (i.e., reacted with) ligand impurities (OD and CH_x) from the HfO_2 film. The formation of SiO_2 after postdeposition annealing was consistent with OD radicals diffusing to the HfO_2/Si interface and oxidizing the substrate silicon, although potential diffusion of O_2 and D_2O from the ambient cannot be completely ruled out. An ultra-thin nitride layer effectively prevented oxygen diffusion and minimized interfacial SiO_2 formation.

Acknowledgment. This work was supported by the National Science Foundation (Grant CHE-0415652) and SEMATECH. L.V.G. and T.G. acknowledge support from the NSF (Grant DMR-0218406). The authors thank Eric L. Garfunkel, Rhett T. Brewer, and Kenneth Bratland for insightful discussions.

CM061761P